Numerical Solution of Fractional Advection-Dispersion Equation

Zhi-Qiang Deng[1]; Vijay P. Singh, F.ASCE[2]; and Lars Bengtsson, F.ASCE[3]

Abstract: Numerical schemes and stability criteria are developed for solution of the one-dimensional fractional advection-dispersion equation (FRADE) derived by revising Fick's first law. Employing 74 sets of dye test data measured on natural streams, it is found that the fractional order F of the partial differential operator acting on the dispersion term varies around the most frequently occurring value of $F=1.65$ in the range of 1.4 to 2.0. Two series expansions are proposed for approximation of the limit definitions of fractional derivatives. On this ground, two three-term finite-difference schemes—"1.3 Backward Scheme" having the first-order accuracy and "F.3 Central Scheme" possessing the F-th order accuracy—are presented for fractional order derivatives. The F.3 scheme is found to perform better than does the 1.3 scheme in terms of error and stability analyses and is thus recommended for numerical solution of FRADE. The fractional dispersion model characterized by the FRADE and the F.3 scheme can accurately simulate the long-tailed dispersion processes in natural rivers.

DOI: 10.1061/(ASCE)0733-9429(2004)130:5(422)

CE Database subject headings: Rivers; Advection; Wave dispersion; Numerical models; Stability analysis.

Introduction

The advection-dispersion equation (ADE) is widely used to solve a range of problems in physical, chemical, and biological sciences, involving dispersion or diffusion, such as mixing in inland and coastal waters (Fischer et al. 1979), transport of thermal energy in a plasma, flow of a chemically reacting fluid from a flat surface, and evolution of populations (Johnson et al. 1995). The fundamental form of the one dimensional (1D) ADE can be expressed as

$$\frac{\partial C}{\partial t}+U\frac{\partial C}{\partial x}=K\frac{\partial^2 C}{\partial x^2} \tag{1}$$

where C=passive scalar (e.g., temperature or concentration of contaminants or dyes); U=mean advective fluid velocity or the drift in the x direction; K=dispersion coefficient; and t=time. Eq. (1) is derived following Fick's first law and in principle it holds after the initial mixing period or for the far field where the longitudinal shear flow dispersion becomes a dominant mechanism of pollutant mixing in rivers.

Analytical solutions of Eq. (1) have been extensively investigated under various initial and boundary conditions. These solutions generally yield a Gaussian spatial distribution or a skewed temporal distribution (both distributions are also called the Fickian solution) for an instantaneous point source (passive) and constant velocity and dispersion coefficient (Rutherford 1994; Fischer et al. 1979). One characteristic of the Gaussian spatial profile solution is that its variance increases proportionally with time and its peak concentration decreases in a manner inversely proportional to the square root of time.

It can be proved that the Fickian temporal peak concentration decays inversely with the square root of distance x and the temporal variance increases proportionally with x as x becomes large (Hunt 1999). However, observations of tracer clouds in rivers have revealed persistent deviations from the behavior predicted by the Fickian solution (Nordin and Troutman 1980). Data collected from nearly 100 streams and rivers show that the unit-peak concentration tends to attenuate in proportion to the travel time with the 0.89 power, not the 0.5 power (Jobson 2001). Day (Hunt 1999) found in 49 different runs that the measured temporal peak concentrations decayed inversely with x^n in which n varied in the range of 0.75–1.59 and had a mean value of 1.17 and a standard deviation of 0.21. Observed values for the variance were proportional to x^m in which m ranged from 1.84 to 2.3 with a mean of 2.06. Fig. 1 shows a typical example of the non-Gaussian temporal distribution from the results of dye tests conducted on the Monocacy River (Nordin and Sabol 1974).

A distinguishing characteristic of the distribution in Fig. 1 is a steep leading edge followed by a flat long tail stretching upstream, demonstrating a greater variance than that of the Fickian solution. On the other hand, to fit the Fickian solution to observed data, Day (Hunt 1999) also found that the dispersion coefficient should be increased indefinitely with distance downstream. In either case the Fickian solution consistently shows a disagreement with laboratory and field data. These results demonstrate that concentration profiles measured in natural media do not follow that predicted by the Fickian theory. This means that the ADE in Eq. (1), based on the classical Fickian law, is not capable of reflecting the long tail dispersion process. A revision of the ADE in Eq. (1)

[1]Assistant Professor, Dept. of Civil and Environmental Engineering, Louisiana State Univ., Baton Rouge, LA 70803-6405; formerly, Research Scholar, Dept. of Water Resources Engineering, Lund Univ., Box 118, S-22100 Lund, Sweden.

[2]A. K. Barton Professor, Dept. of Civil and Environmental Engineering, Louisiana State Univ., Baton Rouge, LA 70803-6405. E-mail: cesing@lsu.edu

[3]Professor, Dept. of Water Resources Engineering, Lund Univ., Box 118, S-22100 Lund, Sweden.

Note. Discussion open until October 1, 2004. Separate discussions must be submitted for individual papers. To extend the closing date by one month, a written request must be filed with the ASCE Managing Editor. The manuscript for this paper was submitted for review and possible publication on May 23, 2002; approved on October 30, 2003. This paper is part of the ***Journal of Hydraulic Engineering***, Vol. 130, No. 5, May 1, 2004. ©ASCE, ISSN 0733-9429/2004/5-422–431/$18.00.

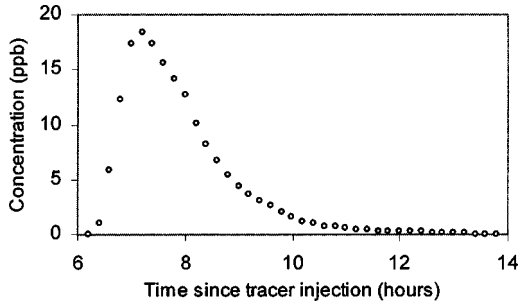

Fig. 1. Non-Gaussian dispersion of tracer in Monocacy River

is necessary for a better simulation of non-Fickian dispersion processes. As a result, extensive efforts have been made to revise the Fickian theory and thus the classical ADE in Eq. (1).

A promising approach for revision of the Fickian theory is the application of fractional derivatives, because they permit a description of continuous time random walks (CTRW) that result in long tail distributions by assigning a joint space-time distribution to individual particle motions (Metzler and Klafter 2000), leading to fractional advection-dispersion equation (FADE). The main advantage of the FADE is that it has solutions which resemble the highly skewed and heavy-tailed breakthrough curves observed in field and whose variance is greater than that of the Gaussian distribution and may grow to be infinite. By modifying Fick's law and using the eigenvector equation and fractional Fokker-Planck equation, Chaves (1998) proposed a symmetrical FADE for isotropic media and an asymmetrical FADE with two different diffusivities for anisotropic media. Fundamental solutions of FADE are Lévy's α-stable distribution. Based on CTRW, Meerschaert et al. (1999) extended the 1D FADE to a multidimensional form with a skewness parameter.

Except for some special initial and boundary conditions, analytical solutions of FADE are difficult to find. In order to make the practical application of FADE available, Benson et al. (2000) took two identical diffusivities in Chaves' FADE or the skewness parameters of Meerschaert's FADE and used the Fourier transform technique to obtain an analytical solution with two symmetrical tails. The FADE approach appears to have the potential for the prediction of non-Fickian dispersion processes, but its wide application is hindered by the difficulty in obtaining analytical solutions, especially when reaction terms are incorporated. Another problem is that shear flow dispersion is not explicitly included in FADEs. All the existing FADEs are derived from the CTRW of molecular particles and thus they are actually just fractional advection-diffusion equations instead of the real fractional advection-dispersion equations. This means that the existing FADEs are only applicable to the diffusion process dominated by molecular random walks. However, the shear velocity-caused dispersion plays a far more important role in actual dispersion processes in turbulent shear flows than does the molecular diffusion (Fischer et al. 1979). In fact, molecular diffusion is negligible as compared to the shear flow dispersion.

Another alternative of the Fickian ADE is the dead-zone models. The very long tails are often attributed to the trapping effect of particles in dead zones (Nordin and Troutman 1980). The dead zone models simulate the heavy tail distribution by artificially adding a reaction (storage-release) term in Eq. (1) and adjusting the reaction parameters to match the observed dispersion distributions (Seo and Cheong 2001). Usually, the dead zone models fit the observed data more closely than does Eq. (1), but they are characterized by a decay in the skewness, which is not displayed by the observed distributions (Nordin and Troutman 1980). Furthermore, the adjusted parameters of the dead zone models appear to be physically unreasonable (Czernuszenko et al. 1998). Hunt (1999) found that the temporal variance and peak concentration decay rate of the dead-zone model have behaviors that are similar to the corresponding results for the Fickian model. In short, the dead zone models are still troublesome in both the goodness of fit and the physical relevance of their parameters. It should be pointed out that some discrepancies between predictions of the 1D models and observations are unavoidable, since the 1D models numerically approximate the real-world phenomena by a one-dimensional numerical algorithm. The fundamental causes of the dispersion processes in natural rivers are velocity shearing of the profile and the storage-release effect of dead-zones.

From the above discussion it can be seen that a sound dispersion model should possess the following characteristics: (1) The variance of the predicted concentration profiles should be much higher than that of the Fickian profiles and thus a fractional advection-dispersion equation should be the best option. (2) The storage-release (reaction) effect is induced by the dispersion process and thus it should be related to the dispersion coefficient K and be either included in the new dispersion term (note: this term in a sound model should be different from the dispersion term in the classical ADE) or produced automatically by the new dispersion term. It is not necessary to artificially add a storage-release (reaction) term in a sound advection-dispersion equation. (3) The new dispersion term can be divided into two parts: The first part should represent the dispersion process in the bulk flow and the second part should be able to reflect the long-range dependence feature of the dispersion process in natural media or the hierarchical release process caused by the dead-zones. The features actually can be employed as qualitative criteria for judging whether a dispersion model is reasonable or not.

The overall goal of this paper is to develop a physically based fractional-order advection-dispersion equation and an efficient numerical scheme for the solution of the equation so that the non-Fickian dispersion processes involved in various fields including natural rivers can be accurately predicted. To that end, the specific objectives are therefore (1) to derive a process-oriented and physically based fractional advection-dispersion equation (FRADE); (2) to develop numerical schemes for FRADE; (3) to determine stability requirements of numerical schemes for different cases; and (4) to demonstrate the application of the FRADE and the new numerical scheme and to test the efficacy of the model.

Fractional Advection-Dispersion Equation

It is essential to understand the mechanisms of dispersion for development of a reasonable ADE, as the ADE is the result of the continuity equation coupled with some kind of a dispersion flux law, such as Fick's law. In general, if there is no significant storage effect of dead zones, a real dispersion process is the combination of three different processes (Fischer et al. 1979): (1) The molecular diffusion or the Fickian diffusion; (2) the turbulent diffusion; and (3) the shear flow dispersion. Of these mechanisms, the molecular diffusion always exists in the transport processes of scalars no matter whether the fluid is in a static state or in a flowing state and is laminar flow or turbulent flow. The turbulent diffusion is usually anisotropic and highly dependent on the involved length and velocity scales. The shear flow dispersion is

induced by the velocity gradients due to the viscosity of the fluid and the resistance of the fluid boundary, and thus it may occur in both laminar and turbulent flow. As compared to the dispersion, the diffusion contribution in the longitudinal direction is negligible. Therefore, this paper mainly focuses on dispersion and advection processes.

Fractional Advection-Dispersion Equation

For the convenience of revision of Fick's first law, Eq. (1) is recast into the following form:

$$\frac{\partial C}{\partial t}+U\frac{\partial C}{\partial x}=\frac{\partial(-J)}{\partial x} \quad \text{and} \quad J=-K_F\frac{\partial^{F-1}C}{\partial x^{F-1}} \tag{2}$$

in which $F=2$ in terms of Fick's first law; J=dispersion flux; and K_F=dispersion coefficient, generally regarded as a constant. It should be noted that the classical Fick's first law with $F=2$ is valid only for isotropic media. Unfortunately, natural media are rarely isotropic and almost fully heterogeneous. For anisotropic media F should be a fraction, including the integer constant of 2 as a special value. Physically, the fractional differential order F represents the heterogeneity of natural media. For instance, in natural rivers and streams there is a wide spectrum of dead-zones, such as reverse flows induced by bends and pools, side pockets, zones between dikes, turbulent eddies, and wakes behind bed irregularities and roughness elements (ripples, sand-dunes, cobbles, boulders, etc.), and so on. The dead-zones are characterized by hierarchical structures that contain pollutant storage-release zones with the size ranging from flow depth to millimeter or even a smaller scale. Pollutants captured by large-scale dead-zones are easily and quickly released but the release processes of pollutants trapped in the small-scale dead-zones may take a long time, causing a hierarchical release of the pollutants and thus the long-tailed dispersion process. Such a hierarchical dead-zone induced scaling dispersion process is difficult to describe by currently available models. However, fractional derivative-based differential equations are found to be particularly suited for describing the long-tailed dispersion processes observed in systems with hierarchical scaling structures (Zaslavsky 2002; Sokolov et al. 2002; Metzler and Klafter 2000). Consequently, to reflect the influence of heterogeneity of the medium and for generality or universality the differential order F in this paper is allowed to be a fraction instead of the integer constant of 2, leading to the following equation:

$$\frac{\partial C}{\partial t}+U\frac{\partial C}{\partial x}=K_F\frac{\partial^F C}{\partial x^F} \tag{3}$$

Eq. (3) reduces to Eq. (1) when $F=2$. Eq. (3) is the FRADE suggested for natural streams. Owing to the importance of parameter F in the dispersion processes and for the convenience of reference, parameter F is termed as ''Fractor'' in this paper. Due to the heterogeneous nature of natural media factor F varies significantly from one medium to another instead of keeping the integer constant 2.

Range of Variation of Fractor F

An understanding of fractor F is essential for development of a numerical method for FRADE and for application of the partial differential equations that are derived directly using Fick's law or in analogy with Fick's law. As mentioned earlier, fractor F may be physically understood as the anisotropic extent of the medium through which the dispersion process occurs. The smaller than 2 is the fractor, the more heterogeneous is the medium. For isotropic media the fractor becomes the integer 2. Employing 74 sets of dye test data collected from the U.S. streams (Yotsukura et al. 1970; Nordin and Sabol 1974) the FRADE (3) was numerically solved and then fractor F was determined by fitting the computed concentrations to the observed concentration distributions. It is shown that (1) fractor F is the controlling factor causing the no-Fickian dispersion in natural streams and (2) fractor F varies in the range from 1.4 to 2.0 around the most frequently occurring value of $F=1.65$, as shown in Fig. 2. In a total of 74 data sets, $F=1.5-1.6$ occurs with a frequency of 20/74; $F=1.6-1.7$ accounts for 21/74; $F=1.7-1.8$ also has a frequency of 20/74; and only one F value falls in the range of 1.9–2.0. This means that all the existing partial differential equations, based on the classical Fick's law directly or indirectly, need to be revised following the new finding that may mark the beginning of a wide application of fractional partial differential equations in hydraulics.

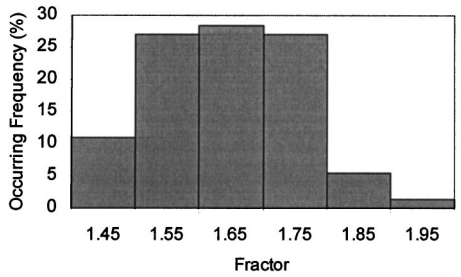

Fig. 2. Occurring frequency distribution of fractor

Numerical Schemes for Fractional Advection-Dispersion Equation

The key to solving FRADE is to properly define the fractional derivatives and to develop a feasible numerical scheme as the fractional-order derivatives are usually characterized by a long-range dependence and they are thus difficult to use in numerical computations. There are different definitions of fractional derivatives. The Grünwald definition and other modified definitions are convenient for numerical solutions. Based on the Grünwald definition of the fractional derivatives, the value of a fractional differential operator acting on the function $C(x,t)$ is an infinite series (Oldham and Spanier 1974), i.e.

$$\frac{\partial^F C(x,t)}{\partial x^F}=\lim_{N\to\infty}\frac{1}{h^F\Gamma(-F)}\sum_{j=0}^{N-1}\frac{\Gamma(j-F)}{\Gamma(j+1)}C(x-jh,t) \tag{4}$$

where $h=\Delta x=x/N$; N=positive integer; and $\Gamma()$=gamma function.

Oldham and Spanier (1974) also presented the following modified Grünwald definition and stated that this definition was superior to Eq. (4) in its convergence properties:

$$\frac{\partial^F C(x,t)}{\partial x^F}=\lim_{N\to\infty}\frac{1}{h^F\Gamma(-F)}\sum_{j=0}^{N-1}\frac{\Gamma(j-F)}{\Gamma(j+1)}C\left(x+\frac{F}{2}h-jh,t\right) \tag{5}$$

This definition calls for evaluation of C at points other than the known C_j values at grid points unless $F=0,\pm 2,\pm 4,\ldots$. It is, therefore, necessary to approximate the definition of Eq. (5) so that all the C values can be evaluated using the C_j values at grid points. The simplest way to do so is to take an integer number as the approximation of $F/2$. It has been found that the F values are

Table 1. Change of Fractional Binomial Coefficients with Memory Length j and Fractor F

Memory length j	Fractor F										
	2.0	1.9	1.8	1.7	1.6	1.5	1.4	1.3	1.2	1.1	1.0
0	1	1	1	1	1	1	1	1	1	1	1
1	−2	−1.9000	−1.8000	−1.7000	−1.6000	−1.5000	−1.4000	−1.3000	−1.2000	−1.1000	−1
2	1	0.8550	0.7200	0.5950	0.4800	0.3750	0.2800	0.1950	0.1200	0.0550	0
3	0	0.0285	0.0480	0.0595	0.0640	0.0625	0.0560	0.0455	0.032	0.0165	0
4	0	0.0078	0.0144	0.0193	0.0224	0.0234	0.0224	0.0193	0.0144	0.0078	0
5	0	0.0033	0.0063	0.0089	0.0108	0.0117	0.0116	0.0104	0.0081	0.0045	0
6	0	0.0017	0.0034	0.0049	0.0061	0.0068	0.0070	0.0064	0.0051	0.0030	0
7	0	0.0010	0.0020	0.0030	0.0038	0.0044	0.0046	0.0043	0.0035	0.0021	0
8	0	0.0006	0.0013	0.0020	0.0026	0.0030	0.0032	0.0031	0.0025	0.0015	0
9	0	0.0004	0.0009	0.0014	0.0018	0.0022	0.0024	0.0023	0.0019	0.0012	0
10	0	0.0003	0.0006	0.0010	0.0014	0.0016	0.0018	0.0018	0.0015	0.0009	0
11	0	0.0002	0.0005	0.0008	0.0010	0.0013	0.0014	0.0014	0.0012	0.0007	0
13	0	0.0001	0.0003	0.0005	0.0006	0.0008	0.0009	0.0009	0.0008	0.0005	0
15	0	0.0000	0.0002	0.0003	0.0004	0.0006	0.0006	0.0007	0.0006	0.0004	0

concentrated in the range of 1.4–2.0 with 1.65 having the highest frequency of occurrence, as shown in Fig. 2. This means that $F/2$ ranges from 0.7 to 1.0 with 0.825 having the highest frequency. Consequently, a fixed integer constant 1 is assumed for $F/2$ when determining C at a grid point. This leads to

$$\frac{\partial^F C(x,t)}{\partial x^F} = \lim_{N\to\infty} \frac{1}{h^F \Gamma(-F)} \sum_{j=0}^{N-1} \frac{\Gamma(j-F)}{\Gamma(j+1)} C(x+h-jh,t) \tag{6}$$

Obviously, the definition of Eq. (6) is based on the Oldham definition of Eq. (5) and Fig. 2.

In analogy with the backward finite-difference expressions of integer-order derivatives, Grünwald-Letnikov gave the following definition of fractional derivatives by induction (Podlubny 1999):

$$\frac{\partial^F C(x,t)}{\partial x^F} = \lim_{N\to\infty} \frac{1}{h^F} \sum_{j=0}^{N} (-1)^j \binom{F}{j} C(x-jh,t) \tag{7}$$

where the fractional binomial coefficients F over j = weighting factors, which reflect the length of the memory of the fractional derivative and can be calculated using the following recurrence relationships or the fast Fourier transform (Podlubny 1999):

$$w_j^F = (-1)^j \binom{F}{j} = \left(\frac{j-1-F}{j}\right) w_{j-1}^F, \quad w_0^F = 1, \quad j = 1,2,3,\ldots \tag{8}$$

Test calculations indicate that the coefficients of C in Eqs. (6) and (7) give identical values for the same F and j. It should be noted that the right-hand side of Eq. (7) is the summation of $N+1$ $(j=0,1,\ldots,N)$ terms, whereas other definitions involve N terms. As the coefficients in Eqs. (4), (6), and (7) are equivalent, these definitions can, therefore, be expressed in the same form

$$\frac{\partial^F C(x,t)}{\partial x^F} = \lim_{N\to\infty} \frac{1}{h^F} \sum_{j=0}^{N} w_j^F C(x-jh,t) \times (\text{Grünwald-Letnikov definition}) \tag{9a}$$

$$\frac{\partial^F C(x,t)}{\partial x^F} = \lim_{N\to\infty} \frac{1}{h^F} \sum_{j=0}^{N+1} w_j^F C(x+h-jh,t) \times (\text{Deng-Singh-Bengtsson definition}) \tag{9b}$$

In order to construct a numerical scheme for fractional derivatives and thereby for fractional differential equations, the two limit definitions of fractional derivatives in Eqs. (9*a*) and (9*b*) are approximated as

$$\frac{\partial^F C(x,t)}{\partial x^F} \approx \frac{1}{h^F} \sum_{j=0}^{N} w_j^F C_{N-j}^n \tag{10a}$$

$$\frac{\partial^F C(x,t)}{\partial x^F} \approx \frac{1}{h^F} \sum_{j=0}^{N+1} w_j^F C_{N+1-j}^n \tag{10b}$$

where superscript n = time t, and j = distance x. Eqs. (10*a*) and (10*b*) will serve as the fundamental basis of the fractional finite-difference method. In order to facilitate numerical computation for practical application of the series in Eqs. (10*a*) and (10*b*), it is helpful to know the variation of the weighting coefficients in the series with the memory length j and with factor F. To that end, coefficients in the above definitions of fractional derivatives are calculated using Eq. (8) and listed in Table 1 and plotted against the memory length j in Fig. 3 for $1 \leqslant F \leqslant 2$.

Both Table 1 and Fig. 3 show that the weighting coefficients decrease rapidly when $j \geqslant 3$. Table 1 illustrates that $w_1 = -F$ always and w_2 decreases from 1 to 0 when F varies from 2 to 1. No matter what value the fractor takes on, the weighting coefficients w_j become very small when $j \geqslant 3$. Fractor F is greater than 1.4 in all the data sets used in this paper. The maximum coefficient w_j is equal to 0.064 when $j=3$, corresponding to $F=1.6$, as indicated in Table 1. This means that the contribution of a single term

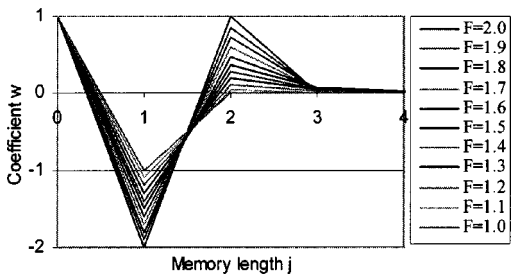

Fig. 3. Variation of fractional binomial coefficients with memory length

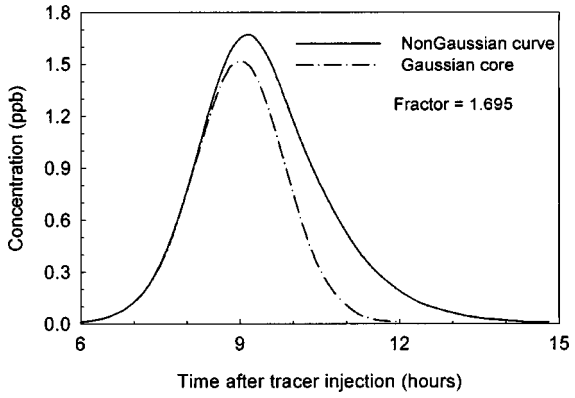

Fig. 4. Comparison between Gaussian core and non-Gaussian tail

becomes negligible to the whole series after $j \geqslant 3$. However, the summation of the terms $j \geqslant 3$ may remain significant especially when the number of the terms is large or the range is long. Such a feature is called the long-range dependence or correlation of fractional derivatives. Anyway, a distinct change of behavior of the series takes place when $j \geqslant 3$. In other words, $j=3$ appears to be a demarcation. To reflect the change, the series in Eqs. (10*a*) and (10*b*) can be expressed in two parts as

$$\frac{\partial^F C}{\partial x^F} \approx \frac{C_m^n - F C_{m-1}^n + w_2^F C_{m-2}^n}{\Delta x^F} + \mathrm{FT}_1$$

$$[w_2^F = F(F-1)/2, \quad m = 1,2,3,\ldots] \tag{11a}$$

$$\frac{\partial^F C}{\partial x^F} \approx \frac{C_{n+1}^n - F C_m^n + w_2^F C_{m-1}^n}{\Delta x^F} + \mathrm{FT}_2 \quad (m = 1,2,3,\ldots) \tag{11b}$$

where

$$\mathrm{FT}_1 = 1/\Delta x^F \sum_{j=3}^{m} w_j^F C_{m-j}^n$$

$$FT_2 = 1/\Delta x^F \sum_{j=3}^{m+1} w_j^F C_{m+1-j}^n$$

The first three terms of the series are called a Gaussian core because for an instantaneous initial condition the numerical solution of FRADE containing the first three terms exhibits a Gaussian distribution, as indicated in Fig. 4 for the case of fractor $F=1.695$. Except for the first three terms, the remaining terms in the series are designated as fractional tail (FT) or non-Gaussian curve since they make the distribution skewed and cause a long tail. It should be noted that the distribution with a long tail and marked by "non-Gaussian curve" in Fig. 4 is the complete numerical solution of FRADE comprising both the non-Gaussian tail part and the Gaussian core part. Actually, the contributions from the core and tail parts vary with time and distance. The farther from the source is the location, the smaller the contribution is from the core part and the greater the contribution is from the tail part, and vice versa. However, numerical experiments reveal that both magnitude and distribution of the non-Gaussian tail are determined by the Gaussian core. Consequently, the Gaussian core is the controlling part of the series but the non-Gaussian tail is the dominant mechanism underlying the long tail distribution or causing the long-range dependence of the dispersion processes in natural media.

It is apparent from Table 1 that Eq. (11*b*) reduces to the forward finite-difference scheme and Eq. (11*a*) to the backward finite-difference scheme when $F=1$. As both the first-order forward scheme and backward scheme have the first-order error, the two schemes (11*a*) and (11*b*) possess the same error order—the first order when $F=1$. When $F=2$, Eq. (11*b*) recovers the second-order central finite-difference scheme and no corresponding scheme can be found for Eq. (11*a*) in the integer-order finite-difference methods. The error order of the schemes (11*b*) and (11*a*) can be analyzed by means of the Taylor series expansion. Using the Taylor expansion and conducting some simple mathematical manipulations yield

$$\frac{\partial^2 C(x)}{\partial x^2} = \frac{C(x+h) - 2C(x) + C(x-h)}{h^2} - \frac{\partial^4 C(x)}{\partial x^4}\frac{h^2}{12} - \cdots \tag{12}$$

$$\frac{\partial^2 C(x)}{\partial x^2} = \frac{C(x) - 2C(x-h) + C(x-2h)}{h^2} + \frac{\partial^3 C(x)}{\partial x^3} h - 7\frac{\partial^4 C(x)}{\partial x^4}\frac{h^2}{12} - \cdots \tag{13}$$

Eq. (12) indicates that the scheme of Eq. (11*b*) possesses the second-order accuracy when $F=2$. It is, therefore, inferred that scheme (11*b*) possesses the F-th order accuracy when $1 \leqslant F \leqslant 2$. It can be seen from Eq. (13) that the scheme of Eq. (11*a*) has the first-order accuracy when $F=2$. It is then inferred that the scheme of Eq. (11*a*) possesses the first-order accuracy when $1 \leqslant F \leqslant 2$. For the convenience of reference, the fractional finite-difference scheme in Eq. (11*b*) is designated as the "F.3 Central Scheme," where "F" means that the scheme is F-th order accurate for the fractional derivative; "3" signifies that the first three terms in the series are used to approximate the main property of the whole series in Eqs. (11*a*) and (11*b*); and "$\cdot$" implies that this is a numerical scheme for fractional derivatives. Likewise, Eq. (11*a*) is termed as the "1.3 Backward Scheme." After an error analysis, the stability requirements of the F.3 Central Scheme and the 1.3 Backward Scheme can be analyzed in conjunction with the fractional advection-dispersion equation (FRADE) [Eq. (3)]. To facilitate manipulation, the first three terms are utilized in the following stability analysis.

von Neumann Stability Analysis of Fractional Numerical Schemes

Stability analysis is utilized to compare the performance and to find the convergent conditions of the above derived fractional finite-difference schemes. Although several methods, such as the energy method, the von Neumann analysis (also called the Fourier series method), and the matrix method, are available for stability analysis, the von Neumann method is relatively simple to apply and provides considerable insight into the performance of different algorithms. Consequently, the von Neumann stability analysis is most widely used. However, this method is local and is only applicable to linear equations with constant coefficients. Therefore, a common assumption made in the von Neumann method is that the coefficients of the difference equations vary so slowly as to be considered constant in space and time. The concept behind the von Neumann analysis is that the finite-difference approximation C_j^n on the lattice $(n\Delta t, j\Delta x)$ of the function $C(t,x)$ is decomposed into convolution of the independent solutions or eigenmodes or harmonics, which are the normalized sine and cosine waves. Each sine/cosine wave is of the form (Press et al. 1988)

$$\xi^n e^{Ik(j\Delta x)} \text{ or } C_j^n = \xi^n e^{Ik(j\Delta x)} \quad (I^2 = -1) \tag{14}$$

where n and j = step numbers in t and x, respectively; k = real spatial wave number; and ξ = complex number which depends on the wave number k and the finite-difference scheme. It is easily found from Eq. (14) that $C_j^{n+1}/C_j^n = \xi$. Therefore, the ratio ξ of C from one time step to the next is the "amplification factor." If $|\xi| \leqslant 1$ for all k, then the Fourier components decay as time is advanced step by step or as they are processed by an iterative solver, the difference scheme is stable. Because of the linear behavior of the Fourier series, it will suffice to consider a single Fourier mode which is a priori generic. To find the amplification factor ξ, the eigenmodes need to be inserted into the scheme. As the stability properties of the pure advection equation have been extensively investigated (Press et al. 1988), this paper only discusses the stability of the pure fractional dispersion equation separated from Eq. (3), i.e.

$$\frac{\partial C}{\partial t} = K_F \frac{\partial^F C}{\partial x^F} \tag{15}$$

Detailed derivations of the stability analysis can be found in the appendix and in Deng (2002).

F.3 Central Scheme for Fractional Dispersion Equation

Explicit Algorithm

Application of the F.3 Central Scheme without the tail part in combination with the forward time scheme to Eq. (15) results in the explicit algorithm of the fractional dispersion equation as

$$C_m^{n+1} = C_m^n + \alpha(C_{m+1}^n - FC_m^n + w_2^F C_{m-1}^n) \quad \left[\alpha = \frac{\Delta t K_F}{(\Delta x)^F}, \quad m = j\right] \tag{16}$$

Inserting the trial solution (14) into Eq. (16) and conducting mathematical manipulations by using some familiar complex number identities yields the stability bound for the explicit F.3 Central Scheme

$$\alpha \leqslant \frac{2}{1 + w_2^F + F} \text{ or } \frac{\Delta t K_F}{(\Delta x)^F} \leqslant \frac{2}{1 + w_2^F + F} \tag{17a}$$

From Table 1 it is seen that $w_2^F = 1$ in case of $F = 2$, resulting in $\alpha \leqslant 1/2$. It implies that

$$\Delta t \leqslant \frac{(\Delta x)^2}{2K_F} \tag{17b}$$

This condition (17b) has been widely used as a stability restriction for the integer-order dispersion equation (Press et al. 1988). Consequently, the inequality of Eq. (17a) is the general stability criterion of the fractional dispersion equation. The physical interpretation of the requirement of Eq. (17a) is that the maximum allowable time step is, up to a numerical factor, the dispersion time across a cell of width Δx. For example, if $F = 1.7$, it is found from Table 1 that $w_2^F = 0.595$. In this case, the time step should be chosen in the range of $\Delta t \leqslant 0.607(\Delta x)^{1.7}/K_F$. The condition in Eq. (17a) is simple, although the process of deriving the inequality is complicated.

Implicit Algorithm

Now, consider the following implicit algorithm of Eq. (15) when the F.3 Central Scheme without the tail part is used.

$$C_m^{n+1} = C_m^n + \alpha[\lambda(C_{m+1}^{n+1} - FC_m^{n+1} + w_2^F C_{m-1}^{n+1}) + (1-\lambda)(C_{m+1}^n - FC_m^n + w_2^F C_{m-1}^n)] \tag{18}$$

in which the weighting factor λ is a chosen number in the interval [0,1]. Carrying out some complex number transforms gives the expression of the amplification factor $|\xi|$ as follows:

$$|\xi| = \frac{|\varphi(1 + w_2^F + F) - 1|}{\beta(1 + w_2^F + F) + 1} \tag{19}$$

Then, consider three special cases of the weighting factor λ. (1) $\lambda = 0$: In this case, the substitution of $\beta = \alpha\lambda = 0$ and $\varphi = \alpha(1 - \lambda) = \alpha$ into Eq. (19) recovers the amplification factor of the explicit case. This is easily found by comparing Eq. (16) with Eq. (18) for $\lambda = 0$. (2) $\lambda = 1$: In this case, substitution of $\beta = \alpha\lambda = \alpha$ and $\varphi = \alpha(1 - \lambda) = 0$ into Eq. (19) yields

$$|\xi| = \frac{1 + \alpha(1 + F + w_2^F)}{[1 + \alpha(1 + F + w_2^F)]^2} = \frac{1}{1 + \alpha(1 + F + w_2^F)} \tag{20}$$

It is apparent that $|\xi| \leqslant 1$ for all α and factor F and the stability is guaranteed under any condition. The F.3 Central Scheme is, therefore, unconditionally stable for $\lambda = 1$. If $F = 2$, $w_2^F = 1$ leads to $|\xi| = 1/(1 + 4\alpha)$. This result is consistent with the existing one of the integer-order dispersion equation (Press et al. 1988). (3) $\lambda = 0.5$: In this case the F.3 Central Scheme corresponds to the Crank-Nicholson method of the integer-order dispersion equation. Substituting $\beta = \alpha\lambda = 0.5\alpha$ and $\varphi = \alpha(1 - \lambda) = 0.5\alpha$ into Eq. (19) yields

$$|\xi| = \frac{|[0.5\alpha(1 + F + w_2^F)]^2 - 1|}{[0.5\alpha(1 + F + w_2^F) + 1]^2} = \frac{|0.5\alpha(1 + F + w_2^F) - 1|}{0.5\alpha(1 + F + w_2^F) + 1} \tag{21}$$

It is obvious that the stability condition $|\xi| \leqslant 1$ holds for all α and F as w_2^F is determined by F. The F.3 Central Scheme is, therefore, also unconditionally stable for $\lambda = 0.5$. If $F = 2$, $w_2^F = 1$ yields $|\xi| = |2\alpha - 1|/(2\alpha + 1)$. This is the stability requirement posed for the integer-order dispersion equation (Press et al. 1988). In general, it can be easily proved that the F.3 Central Scheme is unconditionally stable for $0.5 \leqslant \lambda \leqslant 1.0$ and $\alpha \geqslant 0$. It follows from the above analysis that the F.3 Central Scheme recovers the corresponding central space scheme of the integer-order dispersion equation when $F = 2$.

1.3 Backward Scheme for Fractional Diffusion Equation

Explicit Algorithm

Application of the 1.3 Backward Scheme in conjunction with the forward time scheme to Eq. (15) results in another explicit algorithm of the fractional diffusion equation

$$C_m^{n+1} = C_m^n + \alpha(C_m^n - FC_{m-1}^n + w_2^F C_{m-2}^n) \quad (m = jh) \tag{22}$$

Following the similar procedures and manipulations as the F.3 scheme, the amplification factor $|\xi|$ can be finally expressed in a simple form

$$|\xi| = 1 + \alpha(1 + w_2^F + F) \tag{23}$$

Eq. (23) indicates that the amplification factor $|\xi| \geqslant 1$ always for all values of $\alpha \geqslant 0$ and F. It means that the numerical solution grows as it is dispersed. Consequently, the 1.3 Backward Scheme in the explicit case is absolutely unstable and cannot be used.

Implicit Algorithm

Now, consider the implicit case of the 1.3 Backward Scheme. In this case the numerical algorithm of the pure dispersion Eq. (15) can be written as follows:

$$C_m^{n+1}=C_m^n+\alpha[\lambda(C_m^{n+1}-FC_{m-1}^{n+1}+w_2^FC_{m-2}^{n+1})$$
$$+(1-\lambda)(C_m^n-FC_{m-1}^n+w_2^FC_{m-2}^n)] \quad (24)$$

Following the similar procedures and manipulations as the implicit algorithm of the $F.3$ scheme, the amplification factor $|\xi|$ can be finally expressed as

$$|\xi|=\left|\frac{\varphi(1+w_2^F+F)+1}{\beta(1+w_2^F+F)-1}\right| \quad (25)$$

For $\lambda=0$, Eq. (24) becomes the explicit expression (22). In the meantime, Eq. (25) recovers its counterpart Eq. (23). For $\lambda=0.5$, $\varphi=\beta=0.5\alpha$ and $|\xi|\geqslant 1$ holds always. Therefore, the amplification factor $|\xi|\geqslant 1$ for any value of α and F and the 1.3 Backward Scheme is absolutely unstable in the case of $0\leqslant\lambda\leqslant 0.5$. For $\lambda=1$, $\varphi=0$ and $\beta=\alpha$, Eq. (25) becomes

$$|\xi|=\frac{1}{|\alpha(1+w_2^F+F)-1|} \quad (26)$$

The stability of solution requires $|\xi|\leqslant 1$, i.e.

$$\alpha(1+w_2^F+F)-1\geqslant 1 \quad \text{or} \quad \alpha(1+w_2^F+F)-1\leqslant -1 \quad (27)$$

In Eq. (27), the second inequality is unrealistic. The first inequality leads to the stability limit

$$\alpha\geqslant\frac{2}{1+w_2^F+F} \quad (28)$$

Eq. (28) shows that the 1.3 Backward Scheme is conditionally stable in the implicit case.

The stability analysis further demonstrates that the $F.3$ Central Scheme is indeed more accurate and convenient than the 1.3 Backward Scheme having a narrower range of the α value. Therefore, the $F.3$ central scheme is suggested for the numerical solution of FRADE. Moreover, the results of the stability analysis also show that the existing stability criteria for the pure integer-order dispersion equation are the special cases of that for the pure fractional dispersion equation. Therefore, the stability criteria derived in this paper are the general requirements of stability for both the integer-order and the fractional-order dispersion equations.

Application of the Fractional Dispersion Model to Natural Rivers

A semi-Lagrangian approach (Holly and Preissmann 1977; Karpik and Crockett 1997) is one of the most popular split-operator methods and was thus used in this paper since it solves the advective and diffusive terms of an advection-dispersion equation separately by employing the most efficient method to each term. In the pure advection step, the solution was found by first tracking back the upstream departure point along the characteristic line of the scalar particle and then estimating its concentration at the previous time level by interpolating the known concentration values at the two computational grid nodes bracketing the departure point using cubic spline interpolation.

Since the pure advection process is not subject to any stability limitation on the time step it is desirable to render the pure dispersion process in Eq. (15) unconditionally stable. To that end, the full implicit form of Eq. (18) is used and the fractional tail is added to the equation, leading to

$$-\alpha C_{m+1}^{n+1}+(1+F\alpha)C_m^{n+1}-w_2^F\alpha C_{m-1}^{n+1}$$
$$=C_m^n+\alpha\sum_{nt=0}^{n}\sum_{i=m+2}^{N}w_j^FC_i^{nt} \quad (29)$$

where $m=1,2,3,\ldots,N-1$ and $j=i+1-m$. As all the quantities appearing on the right-hand side are known, Eq. (29) may be simplified by grouping terms as

$$OC_{m-1}^{n+1}+PC_m^{n+1}+QC_{m+1}^{n+1}=R^n \quad (30a)$$

where

$$O=-w_2^F\alpha, \quad P=1+F\alpha, \quad Q=-\alpha$$
$$R=C_m^n+\alpha\sum_{nt=0}^{n}\sum_{i=m+2}^{N}w_j^FC_i^{nt} \quad (30b)$$

For $m=1$ to $N-1$, Eq. (30) can be written as a tridiagonal matrix, a system of simultaneous linear algebraic equations. Therefore, the equations can be efficiently solved using the Thomas Algorithm.

To illustrate the applicability of the above-developed fractional dispersion model (FDM) characterized by the FRADE and the $F.3$ scheme, dye test data, measured on four reaches of the Monocacy River (Nordin and Sabol 1974) and the Missouri River between Sioux City, Iowa, and Plattsmouth, Nebraska (Yotsukura et al. 1970), were employed as these data have relatively high accuracy and were used as typical evidence of the success of the dead (storage) zone model (Czernuszenko et al. 1998; Seo and Cheong 2001). Fig. 5 demonstrates comparisons between the field observed and the model predicted concentration profiles for four reaches of the Monocacy River. Although the first theoretical curve on the left overestimates the values in the initial stage of concentration rise, the agreement between the measurements and the computed curves are excellent in general. Fig. 6 shows comparisons between field dye test data measured on the Missouri River and theoretical dispersion processes simulated by the FDM. The four curves from the left to the right in Fig. 6 correspond to the four observation sections: Decatur Bridge, Blair Bridge, Aksar-ben Bridge, and Plattsmouth Bridge. In terms of the core part or for the main part of a concentration hill, the prediction of the FDM is comparable with or better than the best of the dead-zone

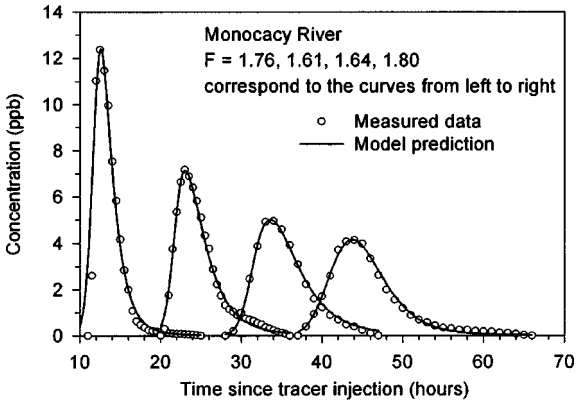

Fig. 5. Comparison between measured and predicted concentration profiles for Monocacy River

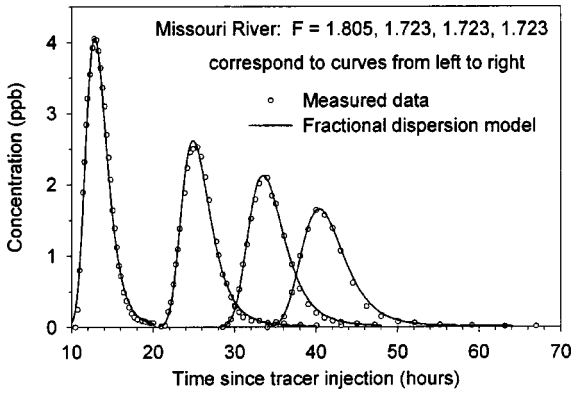

Fig. 6. Comparison between measured and predicted concentration profiles for Missouri River

models. However, the prediction of the FDM is much better than that of the dead-zone model in terms of the long tail.

Furthermore, the FDM has less parameters (two) than do the dead-zone models that have at least four parameters which are allowed to vary. In the above calculations the longitudinal dispersion coefficient K_F is determined by $K_F=(3{,}600K_2)^{F/2}/1{,}609^F$ to maintain the harmony of variable units, where K_F and K_2 carry the dimensions of mile^F/hour and meter^2/second, respectively. K_2 can be determined using the methods proposed by Deng et al. (2001, 2002). For rivers parameter fractor ranges from 1.4 to 2.0. The more heterogeneous the medium is (or the more dead-zones there are in the river), the smaller than 2 is the fractor F. F can be estimated using a moment-based method. Details of the method will be addressed in a future study. It should be emphasized that the contribution from the tail part increases with distance and time, signifying a growing variance in the concentration profile. The FDM gives predictions which are much closer to the observations than the existing dispersion models due to the existence of the long-range dependence part: Non-Gaussian tail in the FDM. Consequently, the FDM fully meets the three qualitative criteria for a sound dispersion model and the results of above comparisons also illustrate its soundness.

Conclusions

The main contribution of the paper lies in the construction of a new numerical algorithm, $F.3$ central finite-difference scheme, and its stability conditions for solving the fractional advection-dispersion equation (FRADE). The FRADE is derived by extending Fick's first law from isotropic media to heterogeneous media and is particularly suitable for description of the highly skewed and heavy-tailed dispersion processes observed in rivers and other natural media. The FRADE is mainly characterized by parameter fractor F acting on the dispersion term. For natural streams, F is in the range of 1.4–2.0. For $1\leqslant F\leqslant 2$, the fractional derivatives can be discretized into two parts: A Gaussian core consisting of the first three terms of the series and a non-Gaussian tail comprised by the remaining terms of the series. With three terms included, the $F.3$ scheme always performs better than the backward scheme 1.3 in terms of error and stability analyses. The existing stability conditions of the integer order dispersion equation are found to be the special cases of the general stability requirements derived for the pure fractional dispersion equation.

The FRADE and the $F.3$ scheme form a new dispersion model, the fractional dispersion model, that captures the main mechanism causing the persistence or the long tail of the dispersion processes in natural media. The fractional dispersion model is a generalized dispersion model and thus can be easily applied to any field where the integer-order advection-dispersion equation is used. The predicted distribution of scalar concentration by the fractional dispersion model matches the observations measured in natural streams quite well if the values of fractor F are properly estimated.

Appendix: Stability Analysis

F.3 Central Scheme for Fractional Dispersion Equation

Explicit Algorithm

Inserting the trial solution (14) into Eq. (16) yields

$$\xi^{n+1}e^{Ik(jh)}=(\alpha e^{Ikh}+(1-\alpha F)+\alpha w_2^F e^{-Ikh})\xi^n e^{Ik(jh)} \quad (31)$$

Eq. (31) leads to

$$\xi=\alpha e^{Ikh}+(1-\alpha F)+\alpha w_2^F e^{-Ikh} \quad (32)$$

To obtain an expression for ξ, the following familiar identities are useful:

$$\frac{e^{I\theta}+e^{-I\theta}}{2}=\cos\theta \quad (33a)$$

$$\frac{e^{I\theta}-e^{-I\theta}}{2I}=\sin\theta \quad (33b)$$

$$1-\cos\theta=2\sin^2\left(\frac{\theta}{2}\right) \quad (33c)$$

$$e^{I\theta}=\cos\theta+I\sin\theta \quad (34a)$$

$$e^{-I\theta}=\cos\theta-I\sin\theta \quad (34b)$$

Substitution of Eqs. (34a) and (34b) with $\theta=kh$ into Eq. (32) leads to

$$\xi=\alpha(\cos kh+I\sin kh)+(1-\alpha F)+\alpha w_2^F(\cos kh-I\sin kh)$$

$$=(1-\alpha F)+\alpha(1+w_2^F)\cos kh+I\alpha(1-w_2^F)\sin kh \quad (35)$$

Since ξ is a complex number, it can be written as

$$\xi=|\xi|(\cos\theta+I\sin\theta) \quad (36)$$

Substituting Eq. (36) into Eq. (35), and equating real and imaginary parts give two expressions for $|\xi|$ and θ in terms of α and h:

$$|\xi|\cos\theta=(1-\alpha F)+\alpha(1+w_2^F)\cos kh \quad (37)$$

$$|\xi|\sin\theta=\alpha(1-w_2^F)\sin kh \quad (38)$$

Squaring and adding Eqs. (37) and (38) result in the mode of the amplification factor ξ:

$$|\xi|^2=[(1-\alpha F)+\alpha(1+w_2^F)\cos kh]^2+[\alpha(1-w_2^F)\sin kh]^2$$

$$=\alpha^2[1+(w_2^F)^2]+(1-\alpha F)^2-2\alpha(1-\alpha F)(1+w_2^F)$$

$$\times[2\sin^2(kh/2)-1]+2w_2^F\alpha^2\{2[2\sin^2(kh/2)-1]^2-1\} \quad (39)$$

Eq. (33c) is employed in deriving Eq. (39). To meet the stability condition $|\xi|\leqslant 1$ for any value of kh, the extreme case of $\sin^2(kh/2)=1$ is considered. In this case, Eq. (39) can be simplified as

$$|\xi|^2=\alpha^2[1+(w_2^F)^2]+(1-\alpha F)^2-2\alpha(1-\alpha F)(1+w_2^F)+2w_2^F\alpha^2 \quad (40)$$

Eq. (40) can be recast into the following simpler form:

$$|\xi|^2=[\alpha(1+w_2^F)-(1-\alpha F)]^2=[\alpha(1+w_2^F+F)-1]^2 \quad (41)$$

The inequality $|\xi|\leq 1$ implies

$$-1\leq\alpha(1+w_2^F+F)-1\leq 1 \quad (42)$$

In Eq. (42), the first inequality is apparent and the second inequality leads to Eq. (17*a*) in the main text.

Implicit Algorithm

Rearranging Eq. (18) so that all $(n+1)$ terms are on the left-hand side and all (n) terms, which are already known, are on the right-hand side

$$-\alpha\lambda C_{m+1}^{n+1}+(1+F\alpha\lambda)C_m^{n+1}-w_2^F\alpha\lambda C_{m-1}^{n+1}=\alpha(1-\lambda)C_{m+1}^n+[1-F\alpha(1-\lambda)]C_m^n+w_2^F\alpha(1-\lambda)C_{m-1}^n \quad (43)$$

Substituting the independent solution of Eq. (14) into Eq. (43) yields

$$[-\alpha\lambda e^{Ikh}+(1+F\alpha\lambda)-w_2^F\alpha\lambda e^{-Ikh}]\xi^{n+1}e^{Ik(jh)}=\{\alpha(1-\lambda)e^{Ikh}+[1-F\alpha(1-\lambda)]+w_2^F\alpha(1-\lambda)e^{-Ikh}\}\xi^n e^{Ik(jh)} \quad (44)$$

Simple manipulation yields

$$\xi=\frac{\varphi e^{Ikh}+[1-F\varphi]+w_2^F\varphi e^{-Ikh}}{-\beta e^{Ikh}+(1+F\beta)-w_2^F\beta e^{-Ikh}} \quad (45)$$

where $\varphi=\alpha(1-\lambda)$ and $\beta=\alpha\lambda$ are introduced. Using Eqs. (34*a*) and (34*b*) with the replacement of $\theta=kh$, Eq. (45) can be rearranged as

$$\xi=\frac{(1-\varphi F)+\varphi(1+w_2^F)\cos kh+I\varphi(1-w_2^F)\sin kh}{(1+\beta F)-\beta(1+w_2^F)\cos kh-I\beta(1-w_2^F)\sin kh} \quad (46)$$

Multiplication of both the numerator and the denominator by the conjugate complex number of the denominator yields

$$\xi=\frac{[(1-\varphi F)+\varphi(1+w_2^F)\cos kh][(1+\beta F)-\beta(1+w_2^F)\cos kh]-\varphi\beta[(1-w_2^F)\sin kh]^2}{[(1+\beta F)-\beta(1+w_2^F)\cos kh]^2+[\beta(1-w_2^F)\sin kh]^2}+I\frac{[(1-\varphi F)+\varphi(1+w_2^F)\cos kh][\beta(1-w_2^F)\sin kh]+[(1+\beta F)-\beta(1+w_2^F)\cos kh][\varphi(1-w_2^F)\sin kh]}{[(1+\beta F)-\beta(1+w_2^F)\cos kh]^2+[\beta(1-w_2^F)\sin kh]^2} \quad (47)$$

Following the same procedure with the derivation of Eq. (39), the mode of the amplification factor $|\xi|$ can be expressed as

$$\begin{aligned}|\xi|^2=&\left\{\frac{(1-\varphi F)(1+\beta F)+(\varphi-\beta+2\beta\varphi F)(1+w_2^F)\cos kh-\varphi\beta[1+(w_2^F)^2]-2\varphi\beta w_2^F(2\cos^2 kh-1)}{(1+\beta F)^2-2\beta(1+\beta F)(1+w_2^F)\cos kh+\beta^2[1+(w_2^F)^2]+2\beta^2 w_2^F(\cos^2 kh-\sin^2 kh)}\right\}^2\\&+\left\{\frac{\beta(1-\varphi F)(1-w_2^F)\sin kh+\varphi(1+\beta F)(1-w_2^F)\sin kh}{(1+\beta F)^2-2\beta(1+\beta F)(1+w_2^F)\cos kh+\beta^2[1+(w_2^F)^2]+2\beta^2 w_2^F(\cos^2 kh-\sin^2 kh)}\right\}^2\\=&\{\langle(1-\varphi F)(1+\beta F)-(\varphi-\beta+2\beta\varphi F)(1+w_2^F)(1-\cos kh-1)-\varphi\beta[1+(w_2^F)^2]\\&-2\varphi\beta w_2^F[2(1-\cos kh-1)^2-1]\rangle/\langle(1+\beta F)^2+2\beta(1+\beta F)(1+w_2^F)(1-\cos kh-1)+\beta^2[1+(w_2^F)^2]\\&+2\beta^2 w_2^F[2(1-\cos kh-1)^2-1]\rangle\}^2\\&+\left\{\frac{(\beta+\varphi)(1-w_2^F)\sin kh}{(1+\beta F)^2+2\beta(1+\beta F)(1+w_2^F)(1-\cos kh-1)+\beta^2[1+(w_2^F)^2]+2\beta^2 w_2^F[2(1-\cos kh-1)^2-1]}\right\}^2\end{aligned} \quad (48)$$

Using Eq. (33*c*) and noting $\theta=kh$ lead to

$$\begin{aligned}|\xi|^2=&\{\langle(1-\varphi F)(1+\beta F)-(\varphi-\beta+2\beta\varphi F)(1+w_2^F)[2\sin^2(kh/2)-1]-\varphi\beta[1+(w_2^F)^2]\\&-2\varphi\beta w_2^F\{2[2\sin^2(kh/2)-1]^2-1\}\rangle/\langle(1+\beta F)^2+2\beta(1+\beta F)(1+w_2^F)[2\sin^2(kh/2)-1]+\beta^2[1+(w_2^F)^2]\\&+2\beta^2 w_2^F\{2[2\sin^2(kh/2)-1]^2-1\}\rangle\}^2\\&+\left\{\frac{(\beta+\varphi)(1-w_2^F)\sin kh}{(1+\beta F)^2+2\beta(1+\beta F)(1+w_2^F)[2\sin^2(kh/2)-1]+\beta^2[1+(w_2^F)^2]+2\beta^2 w_2^F\{2[2\sin^2(kh/2)-1]^2-1\}}\right\}^2\end{aligned} \quad (49)$$

To ensure the stability requirement $|\xi| \leq 1$ for all values of kh, the worst case of $\sin^2(kh/2)=1$ is considered as all other values of $\sin^2(kh/2)$ lead to smaller $|\xi|$ values. The condition of $\sin^2(kh/2)=1$, $\sin(kh)=0$ leads to the disappearance of the second part of Eq. (49). Thus, Eq. (49) can be simplified as

$$|\xi|^2=\left\{\frac{(\varphi-\beta+2\beta\varphi F)(1+w_2^F)+\varphi\beta(1+w_2^F)^2-(1-\varphi F)(1+\beta F)}{(1+\beta F)^2+2\beta(1+\beta F)(1+w_2^F)+\beta^2(1+w_2^F)^2}\right\}^2=\frac{|[\varphi(1+w_2^F+F)-1][1+\beta(1+w_2^F+F)]|}{[1+\beta(1+w_2^F+F)]^2} \tag{50}$$

The simplest form of $|\xi|$ is expression (19) in the main text.

Notation

The following symbols are used in this paper:

- C = passive scalar (e.g., concentration of pollutants);
- F = fractor (fractional differential order of the dispersion term);
- h = distance step ($=\Delta x$);
- J = flux of dispersion;
- K = dispersion coefficient;
- O,P,Q = lower, main, and upper diagonals of the coefficient matrix;
- R = right-hand side of the linear algebraic equation system;
- t = time;
- U = flow velocity;
- w_j^F = series coefficient;
- x = distance along the flow direction;
- α,β,φ = numerical constants;
- Δt = time step;
- Δx = distance step;
- λ = weighting factor; and
- ξ = amplification factor.

References

Benson, D. A., Wheatcraft, S. W., and Meerschaert, M. M. (2000). "The fractional-order governing equation of Levy motion." *Water Resour. Res.*, 36(6), 1413–1423.

Chaves, A. S. (1998). "A fractional diffusion equation to describe Lévy flights." *Phys. Lett. A*, 239(1-2), 13–16.

Czernuszenko, W., Rowinski, P. M., and Sukhodolov, A. (1998). "Experimental and numerical validation of the dead-zone model for longitudinal dispersion in rivers." *J. Hydraul. Res.*, 36(2), 269–280.

Deng, Z.-Q. (2002). "Theoretical investigation into longitudinal dispersion in natural rivers." PhD dissertation, Lund Univ., Lund, Sweden.

Deng, Z.-Q., Bengtsson, L., Singh, V. P., and Adrian, D. D. (2002). "Longitudinal dispersion coefficient in single-channel streams." *J. Hydraul. Eng.*, 128(10), 901–916.

Deng, Z.-Q., Singh, V. P., and Bengtsson, L., (2001). "Longitudinal dispersion coefficient in straight rivers." *J. Hydraul. Eng.*, 127(11), 919–927.

Fischer, H. B., List, E. J., Koh, R. C. Y., Imberger, J., and Brooks, N. H. (1979). *Mixing in inland and coastal waters*, Academic, New York, 30–138.

Holly, F. M., Jr., and Preissmann, A. (1977). "Accurate calculation of transport in two-dimensions." *J. Hydraul. Div., Am. Soc. Civ. Eng.*, 103(11), 1259–1277.

Hunt, B. (1999). "Dispersion model for mountain streams." *J. Hydraul. Eng.*, 125(2), 99–105.

Jobson, H. E. (2001). "Predicting river travel time from hydraulic characteristics." *J. Hydraul. Eng.*, 127(11), 911–918.

Johnson, A. R., Hatfield, C. A., and Bruce, B. T. (1995). "Simulated diffusion dynamics in river networks." *Ecol. Modell.*, 83, 311–325.

Karpik, S. R., and Crockett, S. R. (1997). "Semi-Lagrangian algorithm for two-dimensional advection-diffusion equation on curvilinear coordinate meshes." *J. Hydraul. Eng.*, 123(5), 389–401.

Meerschaert, M. M., Benson, D. A., and Bäumer, B. (1999). "Multidimensional advection and fractional dispersion." *Phys. Rev. E*, 59(5), 5026–5028.

Metzler, R., and Klafter, J. (2000). "The random walk's guide to anomalous diffusion: A fractional dynamics approach." *Phys. Rep.*, 339, 1–77.

Nordin, C. F., and Sabol, G. V. (1974). "Empirical data on longitudinal dispersion in rivers." *Water resources investigations 20–74*, U.S. Geological Survey, Federal Center, Colo.

Nordin, C. F., and Troutman, B. M. (1980). "Longitudinal dispersion in rivers: The persistence of skewness in observed data." *Water Resour. Res.*, 16(1), 123–128.

Oldham, K. B., and Spanier, J. (1974). *The fractional calculus*, Academic, New York.

Podlubny, I. (1999). *Fractional differential equations*, Academic, San Diego.

Press, W. H., Flannery, B. P., Teukolsky, S. A., and Vetterling, W. T. (1988). *Numerical recipes*, Cambridge University Press, New York, 615–666.

Rutherford, J. C. (1994). *River mixing*, Wiley, Chichester, U.K.

Seo, I. W., and Cheong, T. S. (2001). "Moment-based calculation of parameters for the storage zone model for river dispersion." *J. Hydraul. Eng.*, 127(6), 453–465.

Sokolov, I. M., Klafter, J., and Blumen, A. (2002). "Fractional kinetics." *Phys. Today*, 55(11), 48–54.

Yotsukura, N., Fischer, H. B., and Sayre, W. W. (1970). "Measurement of mixing characteristics of the Missouri River between Sioux City, Iowa, and Plattsmouth, Nebraska." *Water-supply paper 1899-G*, U.S. Geological Survey, Federal Center, Colo.

Zaslavsky, G. M. (2002). "Chaos, fractional kinetics, and anomalous transport." *Phys. Rep.*, 371(6), 461–580.